The $FT^{\Lambda} - FR^{\Lambda}$ AWG Network: A Practical Single-Hop Metro WDM Network for Efficient Uni- and Multicasting

Chun Fan Stefan Adams Martin Reisslein

Abstract

Single-hop WDM networks with a central Passive Star Coupler (PSC), as well as single-hop networks with a central Arrayed-Waveguide Grating (AWG) and a single transceiver at each node, have been extensively studied as solutions for the quickly increasing amounts of unicast and multicast traffic in the metropolitan area. The main bottlenecks of these networks are the lack of spatial wavelength reuse in the studied PSC based networks and the single transceiver in the studied AWG based metro WDM networks. In this paper we develop and evaluate the $FT^{\Lambda} - FR^{\Lambda}$ AWG network, which is based on a central AWG and has arrays of fixed-tuned transmitters and receivers at each node. Transceiver arrays are a mature technology, making the proposed network practical. In addition, the transmitter arrays allow for high speed signaling over the AWG while the receiver arrays relieve the receiver bottleneck arising from multicasting in conjunction with spatial wavelength reuse on the AWG. Our results from probabilistic analysis and simulation indicate that the $FT^{\Lambda} - FR^{\Lambda}$ AWG network gives particularly good throughput-delay performance for a mix of unicast and multicast traffic.

Keywords

Arrayed-waveguide grating; medium access control; multicast; single-hop network; throughput-delay performance; transceiver array.

I. Introduction

With the quickly increasing speeds in the local access networks (due to Gigabit Ethernet and similar emerging technologies) and the provisioning of very-high capacity backbone WDM networks, the metropolitan area networks are becoming a bottleneck—the so called metro-gap. This is largely due to the current circuit-switched SONET/SDH over WDM metro networks, which carry the increasing amount of bursty data and multimedia traffic inefficiently. This situation is further exacerbated by the placement of content distribution proxies in the metro area and the emergence of peer-to-peer networking paradigms. These developments will further increase the traffic load on metro networks. In addition, there will likely be an increase in the portion of multicast (multi-destination) traffic in the metro area due to the applications supported by the proxy servers and peer-to-peer networks, such as multimedia stream distribution, distributed games, teleconferences, and tele-medicine. Therefore, there is an urgent need for innovative and practical metro networks [1].

A shorter preliminary version of this paper appears in *Proceedings of IEEE Infocom 2004*.

Please direct correspondence to M. Reisslein.

C. Fan and M. Reisslein are with the Dept. of Electrical Eng., Arizona State University, Tempe, AZ 85287–5706, phone: 480–965–8593, fax: 480–965–8325, Email: {chun.fan, reisslein}@asu.edu, Web: http://www.fulton.asu.edu/~mre.

Stefan Adams is with the Dept. of Mathematics, Technical University Berlin, 10623 Berlin, Germany, Email: adams@math.tu-berlin.de.

Supported in part by National Science Foundation through grant Career ANI–0133252 and the DFG research center Mathematics for Key Technologies (FZT86) in Berlin.

Single-hop WDM networks with their minimum hop distance of one (i.e., no bandwidth devoted to multi-hop packet forwarding) and inherent transparency have attracted a great deal of attention as solutions for the metropolitan area. Single-hop WDM networks are typically either based on a central Passive Star Coupler (PSC) or a central Arrayed-Waveguide Grating (AWG). Each wavelength on the PSC provides a broadcast channel from a given PSC input port to all output ports. Thus, the number of simultaneous transmissions in a PSC network is limited by the number of available wavelengths. Generally, wavelengths are precious, especially for the cost sensitive metro area and should be utilized efficiently. For this reason, AWG based networks have recently begun to attract significant attention. The AWG is a wavelength routing device which allows for spatial wavelength reuse, i.e., the entire set of wavelengths can be simultaneously applied at each AWG input port without resulting in collisions at the AWG output ports. This spatial wavelength reuse has been demonstrated to significantly improve the network performance for a fixed set of wavelengths compared to PSC based networks [2], [3].

As detailed in Section I-A, the studied AWG based metro WDM networks employ a single fast-tunable transmitter and a single fast-tunable receiver (TT–TR) at each network node. While this TT–TR node architecture is conceptually very appealing and has a number of advantages, such as low power consumption and small foot print, fast-tunable transceivers are generally a less mature technology than fixed-tuned transceiver arrays. More specifically fast-tunable transmitters have just recently been experimentally proven to be feasible in a cost-effective manner [4], while fast tunable optical filter receivers with acceptable channel crosstalk remain a technical challenge at the photonics level. Overall, arrays of fixed-tuned transmitters and receivers are better understood [5], [6], more mature, more reliable, and commercially available, but also have some drawbacks such as increased power consumption and larger footprint. At the MAC protocol level, transceiver arrays have a number of distinct advantages. The transmitter arrays allow for high-speed signaling over the AWG in contrast to the low-speed signaling through the spectral slicing of broadband light sources [2], [3] which suffer from a small bandwidth-distance product. The receiver arrays, on the other hand, relieve the receiver bottleneck caused by multicast traffic, that is transmitted over the large number of wavelength channels obtained from spatial wavelength reuse on the AWG.

In this paper we develop and evaluate the $FT^{\Lambda} - FR^{\Lambda}$ AWG network, an AWG based single-hop WDM network with an array of fixed-tuned transmitters and receivers at each network node. The proposed $FT^{\Lambda} - FR^{\Lambda}$ AWG network is practical due to its mature, commercially available building blocks. As we demonstrate through analysis and simulation, the network efficiently supports unicast and multicast traffic. The $FT^{\Lambda} - FR^{\Lambda}$ node architecture, aside from being readily deployable, achieves good throughput-delay performance especially for a mix of unicast and multicast traffic.

This paper is organized as follows. In the following subsection we review related work. In Section II, we describe the architecture of the $FT^{\Lambda} - FR^{\Lambda}$ AWG network and discuss how it supports unicast and multicast traffic. In Section III we provide the distributed medium-access-control (MAC) protocol. In Section IV, we develop a probabilistic model to evaluate the throughput-delay performance of the network for a mix of unicast and multicast traffic. This analysis considers an operation of the network with essentially no packet drops, achieved with sufficiently large (electronic) node buffers, and is based on a virtual buffer model of the network. In Section V we present numerical

throughput-delay results obtained from our analytical model and simulations. In Section VI we study the node buffer dimensioning for the network and demonstrate that small node buffers are sufficient to achieve minuscule drop probabilities. We summarize our findings in Section VII.

A. Related Work

Both unicasting (see surveys [7], [8]) and multicasting (see for instance [9]–[22] as well as surveys [23], [24], [25]) over Passive Star Coupler (PSC) based networks have been studied extensively. The studied PSC based networks include networks with arrays of fixed-tuned receivers (see for instance [26]), as well as networks with arrays of fixed-tuned transmitters and receivers (see for instance [27]). The key bottleneck in the PSC based network is the channel resource limitation due to the lack of spatial wavelength reuse.

Recently, the use of the wavelength routing AWG as the central hub in single-hop networks has received more attention. The spatial wavelength reuse of the AWG overcomes the channel resource limitations of single hop PSC based networks. The photonic feasibility aspects of the single-hop WDM networks based on a uniform-loss cyclic-frequency AWG with nodes consisting of individual transceivers as well as transceiver arrays have been demonstrated in [28], [29]. General design principles for networks based on AWGs are studied, for instance, in [30]–[41].

SONATA [42], [43] is a national-scale network based on an AWG. In SONATA, individual nodes (terminals) are connected to passive optical networks (PONs) which in turn are connected to the AWG. SONATA employs a centralized network controller to arbitrate the access of the terminals to the shared wavelength channels and wavelength converter arrays at the central AWG to balance the load between PON pairs. In contrast, we consider a metropolitan area network in this paper with decentralized medium access control. Our network is completely passive and does not employ any wavelength converters.

Unicasting and multicasting in a single-hop AWG based metro WDM network with decentralized media access control are also studied in [2], [3]. The network considered in [2], [3] employs a single fast-tunable transmitter and a single fast-tunable receiver (TT–TR) at each node, which results in slow signalling and the receiver bottleneck. We also note that the analytical performance model of the multicasting in the TT–TR AWG network developed in [3] considers a simplified multicast traffic model in which a multicast packet is destined to all nodes attached to exactly one of the AWG output ports. In contrast, we develop in this paper an analytical performance model for the multicasting in the $FT^{\Lambda}-FR^{\Lambda}$ AWG network which considers the more realistic and widely accepted multicast traffic model with randomly uniformly distributed number and location of destinations of a multicast packet.

We remark that we focus on the network and MAC protocol design of the $FT^{\Lambda} - FR^{\Lambda}$ AWG network and its performance evaluation in this paper. The protection and survivability aspects of the network are beyond the scope of this paper. We note that protection strategies for AWG based networks have been examined in [44], [45], [46]. In our ongoing work we are developing similar strategies for the $FT^{\Lambda} - FR^{\Lambda}$ network.

II. Architecture

Our AWG based network architecture is illustrated in Fig. 1. The AWG has D input ports and D output ports. There are N nodes in the network. At each AWG input port, an $S \times 1$, $S = N/D$, combiner collects transmissions from the transmitters of S attached nodes. At each AWG output port, a $1 \times S$ splitter equally distributes the signal to S individual fibers that are attached to the receivers of the nodes. We use the notation $N_{i,j}$, $i = 1, 2, \ldots, D$, $j = 1, 2, \ldots, S$, to designate the jth node attached to the ith AWG port. In Fig. 1, $T_{i,j}$ and $R_{i,j}$ correspond to the transmitter array and the receiver array of node $N_{i,j}$.

The wavelength routing property of the AWG is illustrated in Fig 2 for a 2×2 AWG with a period of the wavelength response (referred to as Free Spectral Range (FSR)) of $R = 2$. According to the periodic wavelength routing, every second wavelength is routed to the same AWG output port. Note that two transmissions on different wavelengths are required to reach both AWG output ports from a given input port. Also note that $\Lambda = D \cdot R$ wavelength channels can be simultaneously used at each of the D AWG ports without resulting in channel collisions. With this "spatial reuse" of wavelength channels, the AWG provides a total of $D \cdot \Lambda$ channels from its D input ports to its D output ports. There are R channels between each input-output port pair.

The node architecture is shown in Fig. 3. Each node is equipped with a transmitter array consisting of Λ fixed tuned transmitters and a receiver array consisting of Λ fixed tuned receivers. The optical multiplexer is used to combine multiple transmissions from the node's transmitter array onto the transmission fiber. The optical demultiplexer is used to separate the signal from the receiving fiber to the receiver array.

We close this overview of the $FT^{\Lambda} - FR^{\Lambda}$ AWG network architecture by noting its implications on the transmission of unicast and multicast packets. A unicast packet, i.e., a packet that is destined to one destination node, requires one transmission on the wavelength that is routed to the AWG output port that the destination node is attached to.

Now consider a multicast packet, i.e., a packet that is destined to two or more destination nodes. If all destination nodes are attached to the same AWG output port, then only one transmission is required on the wavelength routed to that AWG output port. The splitter locally broadcasts the transmission to all attached nodes, including the intended destination nodes. On the other hand, if the destination nodes of a given multicast packet are attached to different AWG output ports, transmissions on multiple wavelengths routed to the different AWG output ports are required. As

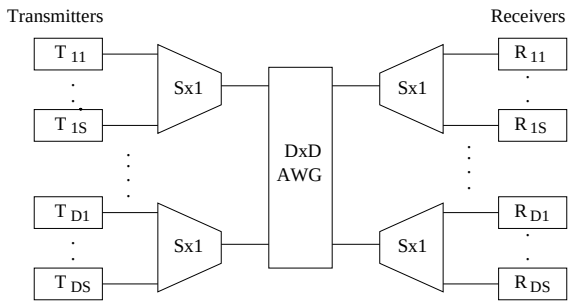

Fig. 1. Network architecture

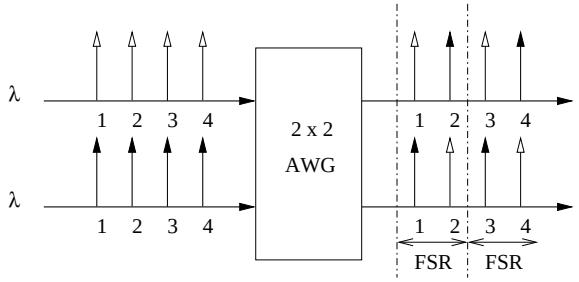

Fig. 2. Wavelength routing in 2×2 AWG with $R = 2$ FSRs

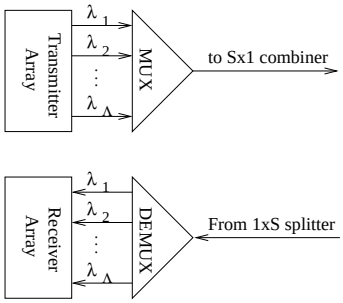

Fig. 3. Detailed node architecture

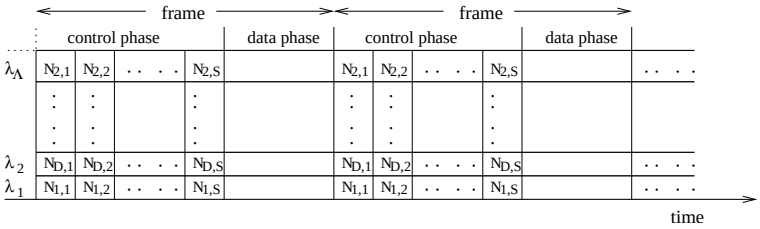

Fig. 4. Frame structure and control packet reception schedule for nodes at AWG output port 1 of network with $R = 1$ FSR

discussed in the next section in more detail, these multiple transmissions can be conducted in parallel using multiple transmitters in the source node's transmitter array at the same time.

III. MAC Protocol

In this section we develop a MAC protocol employing pre-transmission coordination together with global scheduling to coordinate the access of the nodes to the shared wavelength channels in the $FT^{\Lambda} - FR^{\Lambda}$ AWG network. This coordination and scheduling are generally recommended strategies for achieving good throughput-delay performance in shared-wavelength single-hop star networks [7]. Time is divided into frames; each frame consists of a control phase and a data phase, as illustrated in Fig. 4. The length of each control packet measured in time is one slot. One control packet is generated for each data packet. The control packet contains the address of the destination node for unicast packets or the multicast group address for multicast packets.

We develop two control packet transmission strategies: time-division multiple access (TDMA) and contention similar to slotted Aloha. With either strategy, the periodic wavelength routing property of the AWG requires a transmitting node to use all of the wavelengths covering at least one FSR in order to reach all of the AWG output ports. The spatial wavelength reuse property also allows nodes attached to different ports of the AWG to use the same set of wavelengths without channel collision.

A. TDMA control packet transmission

The TDMA sequence for control packet transmission in an AWG network with *one* FSR ($R = 1$) is as follows: In the first slot of the control phase, one node from each input port of the AWG, say the first node $N_{d,1}$ at each port $d = 1, 2, \ldots, D$, transmits its control packet. Each node uses its full array of fixed transmitters for high-speed control packet transmission (in contrast to the lower speed signaling with spreading and spectral slicing employed in the single transceiver network [2], [3]). In the second slot, another node from each AWG input port, say the second node $N_{d,2}$ at each port $d = 1, 2, \ldots, D$, transmits its control packet. This continues until all of the nodes have transmitted their control packets. Fig. 4 shows the corresponding control packet reception schedule by the receiver array of the nodes at AWG output port 1, the reception schedules for the other output ports are analogous. Note that the control packets do not need to carry the source address, as the source node address can be inferred from the reception schedule. The control phase is S slots long. (Recall that $S = N/D$ and $\Lambda = D \cdot R$. In the considered case $R = 1$ we have $\Lambda = D$ and thus

$S = N/\Lambda$.)

In the case of a network with R FSRs, we split the nodes attached to each AWG port into R subgroups. Each subgroup is given a different FSR for the transmission of the control packets. Thus we have R nodes from each input port simultaneously transmitting control packets, each node using all wavelengths in one of the R FSRs. The control packet reception schedule for the nodes at AWG output port 1 of a $R = 2$ FSR network is shown in Fig. 5.

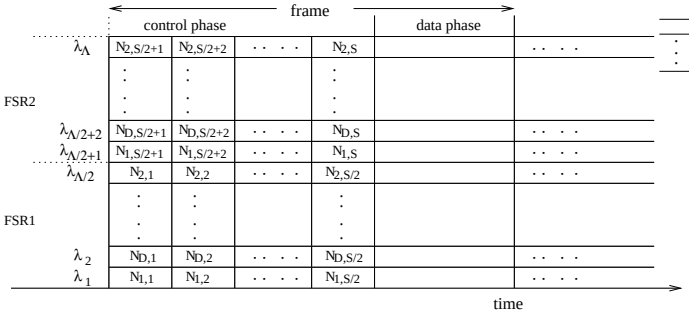

Fig. 5. Frame structure and control packet reception schedule for nodes at AWG output port 1 of network with $R = 2$ FSRs

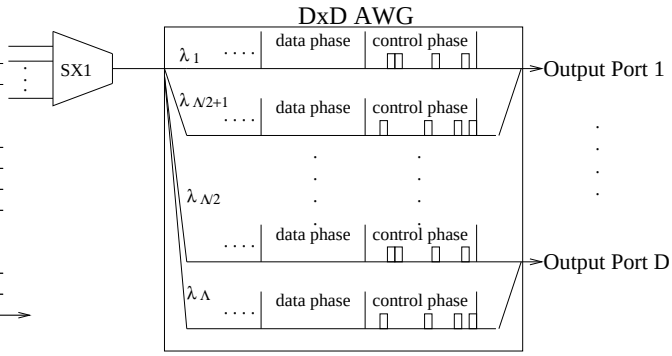

Fig. 6. Control packet contention and frame structure for network with $R = 2$ FSRs; the control phase is M slots long

In general, the length of the control phase with the TDMA transmission strategy is S/R slots. Note however that $S = N/D$ and $R = \Lambda/D$ results in a constant control phase length of N/Λ slots, independent of the number of FSRs R. In other words, the length of the control phase depends only on the number of nodes N and the number of transceivers Λ at each node. Consequently, in our performance evaluations in Section V we do not need to explicitly include the control phase when considering scenarios with TDMA control packet transmission with fixed N and Λ. When comparing scenarios with different TDMA control phase lengths N/Λ or control packet contention, we take the different lengths of the control phase into consideration.

B. Control Packet Transmission with Contention

With the contention control packet transmission strategy, the control packets are transmitted similar to slotted Aloha. In a network with $R = 1$ FSR, each node sends the control packet uniformly and randomly in one of the slots of the M, $M \leq N/\Lambda$, slot long control phase using its full array of transmitters. In the case of multiple FSRs connecting each input-output port pair, the transmitting node picks from one of the FSRs randomly and uniformly to transmit the control packet in a uniformly randomly chosen slot on all wavelengths in the selected FSR, as illustrated in Fig. 5 for $R = 2$.

A collision occurs when two or more nodes select the same control slot (in the same FSR). Since the transmitter uses all the wavelength of one full FSR and the receiver arrays cover all of the wavelengths, the transmitting node knows the results of control contention after a delay of the one-way end-to-end propagation delay. The nodes with collided control packets retransmit the control packet in the following frame.

Note that for the control packet contention, the control packet need to contain the address of the source node in addition to the addresses of the destination nodes.

We also note that in the $FT^{\Lambda} - FR^{\Lambda}$ AWG network, the R wavelengths (and corresponding receivers) connecting a given AWG input port with a given AWG output port are only shared by the transmissions between nodes attached to these two ports. Thus, the network allows for the development of contention based MAC protocols where control packets are only sent to the AWG output port(s) with attached receivers. Such protocols would have the advantage that typically fewer lasers are required for a control packet transmission compared to our protocol where control packets are transmitted to all output ports using all lasers in one FSR. One drawback of such protocols would be that the sending node does not necessarily receive a copy of a sent control packet. Thus, explicit acknowledgements would be required to verify whether a control packet collision occurred; these acknowledgements would result in increased protocol complexity and delay. Along the same line, the $FT^{\Lambda} - FR^{\Lambda}$ AWG network allows for the development of MAC protocols where the data packets content directly for the R wavelength channels connecting a given AWG input-output port pair without pre-transmission coordination. Such uncoordinated data packet contention however would tend to result in a significant waste of bandwidth due to data packet collisions [7].

C. Data Packet Scheduling

Once the control packets of a given control phase are received, all nodes execute the same scheduling algorithm. For a unicast packet, as well as for a multicast packet with all destination nodes attached to one AWG output port, a single packet transmission is scheduled. For a multicast packet with destination nodes at multiple AWG output ports, multiple packet (copy) transmissions are scheduled: one copy is transmitted to each AWG output port with attached multicast destination nodes. For each unicast and multicast packet (copy) transmission, a wavelength is assigned on a first-come-first-served (FC–FS) basis starting with the lowest FSR in the immediate frame. We adopt the FC–FS scheduling since scheduling algorithms for high-speed WDM networks need to be of low complexity [17]. If the FSRs of the immediate frame are scheduled, then slots in the subsequent frame are assigned, and so on, up to a pre-specified scheduling window. If the data packet corresponding to a control packet can not be scheduled within the scheduling window, the control packet fails. The sending node is aware of the failed control packet as it executes the same scheduling algorithm and retransmits the failed control packet in the next frame. Note that unfairness among the nodes may arise with the FC–FS scheduling if the control packets are transmitted (and received) in the fixed TDMA sequence. To overcome this problem, the received control packets can be randomly resequenced before the scheduling commences. Control packet contention also ensures fairness since the control packets are transmitted in randomly selected slots.

Note that the data packets are buffered in the electronic domain at each source node which can have quite large memory capacity. An arriving packet that finds the node buffer full is dropped and is indicative of congestion. We leave traffic congestion management to the upper layer protocols.

IV. Throughput-Delay Analysis Based on Virtual Queue Model

In this section we develop a probabilistic virtual queue based model to evaluate the throughput-delay performance of the $FT^{\Lambda} - FR^{\Lambda}$ AWG network. We assume in this model that the nodal buffers are sufficiently large (infinite in the model) such that only a negligible fraction of the packets is dropped. We demonstrate in Section VI that a reasonably small packet buffer at each node is sufficient to achieve packet drop rates of 10^{-2} and less, which in turn implies a correspondingly small modelling error due to the infinite buffer assumption. We also note that throughout we study the network for stable operation, as detailed in Section IV-D.

A. Overview of Virtual Queue Network Model

We model each AWG input-output port pair as a "virtual" queue. This queue is virtual because there is *no* electronic buffer or optical memory at the AWG. The queue only exists in the electronic memory domain of each node. These virtual queues are illustrated in Fig. 7. The service capacity for a given virtual queue is the number of FSRs R, with each FSR providing a deterministic service rate of one packet per frame.

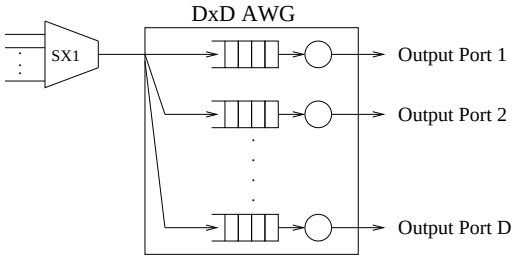

Fig. 7. Queuing model: one *virtual* queue for each AWG input-output port pair. Note that there is no physical buffer at the AWG.

We consider the following scenario in our modelling of the $FT^{\Lambda} - FR^{\Lambda}$ AWG network in this section.

- *Bernoulli traffic arrival*: Each node generates a new data packet with probability σ at the beginning of each frame. A given newly generated packet is a unicast packet with probability u and a multicast packet with probability $1 - u$. Let $\sigma_u = \sigma \cdot u$ denote the probability that a new unicast packet is generated in a given frame and let $\sigma_m = \sigma \cdot (1 - u)$ denote the probability that a new multicast packet is generated in a given frame.
- *Uniform distribution of traffic*: The destination node(s) of a given unicast (multicast) packet are uniformly distributed over all N nodes, including the sending node for mathematical convenience. (Our simulations, which do not allow a node to send to itself, indicate that this simplifying assumption has negligible impact.)
- *Uniform multicast size distribution*: We let Γ, $2 \leq \Gamma \leq N$, represent the maximum number of destination nodes of the multicast packets. The number of destination nodes of a given multicast packet is a random variable γ with $2 \leq \gamma \leq \Gamma$, which is uniformly distributed, i.e., $\gamma \sim U(2, \Gamma)$.
- *Propagation delay*: We initially assume that the propagation delay is negligible. In Section IV-F we discuss how to incorporate propagation delay in our model.

• *Fixed packet size*: We assume that the data packets are fixed in size. The packet size is such that exactly one data packet fits into the data phase of a given frame.
• *TDMA control packet transmission*: We initially focus on the TDMA control packet transmission. The control packet transmission with TDMA and contention are compared in Section V-G.
• *Infinite nodal buffers and scheduling window*

To model the multiple transmissions of copies of a multicast packet destined to multiple AWG output ports, we place one packet copy into each corresponding virtual queue. Thus for a multicast packet from a given AWG input port destined to all D AWG output ports, one packet copy is placed in each of the D virtual queues modelling these D input-output port pairs.

B. Definition of Performance Metrics

In our throughput-delay performance evaluation, we consider the following metrics:
• The *multicast throughput* Z_M is defined as the average number of packet transmissions completed per frame in steady state. The transmission of a multicast packet is complete if all copies of the packet have been delivered.
• The *transmitter throughput* Z_T is defined as the average number of packet (copy) transmissions per frame in steady state.
• The *receiver throughput* Z_R is defined as the average number of packets received by their intended destination nodes per frame in steady state. Each intended destination node of a multicast packet copy transmission counts toward the receiver throughput. A given multicast packet copy transmission can result in up to S received packets in case all nodes attached to the splitter are intended destinations.
• The *delay* W_M is the average time in steady state in frames between the following two epochs: (i) the end of the control phase of the frame in which a packet is generated, and (ii) the beginning of the data phase in which the *last* copy of the packet is transmitted.
• The *copy delay* W_{TR} is defined similar to the delay W_M and is the average time between packet generation and the beginning of the transmission of *any given (arbitrary)* copy of the packet.

Note that when only unicast traffic is considered, $Z_M = Z_T = Z_R$ and $W_M = W_{TR}$. Also note that all of these performance metrics are defined with respect to the frame as elementary time unit. This is convenient as for most of our performance studies we consider a network with fixed number of nodes N and fixed number of transceivers Λ per node. For this network, the length of the TDMA control phase N/Λ is constant, which in conjunction with the fixed data phase (data packet size) results in a constant frame length. Toward the end of our performance evaluation, we will study networks with different N and Λ as well as control packet contention and consequently different frame lengths. For those studies we will modify the above definitions and use the slot as elementary time unit. In addition, for all experiments using the slot as time unit, we define the delay as the average period between the packet generation (at the beginning of a frame) and the beginning of the packet transmission, which includes the duration of the control phase.

C. Number of Packet Copies

In this section we evaluate the number of packet copy transmissions required to service a given generated packet. Let Δ be a random variable denoting the number of AWG output ports (virtual queues) that lead to destination nodes of a given generated packet. In other words, Δ denotes the number of packet copies that are placed in different virtual queues for a given generated packet. A single packet copy is transmitted if either (i) the generated packet is a unicast packet (which has probability u), or (ii) the generated packet is a multicast packet (which has probability $1-u$) and all the destination nodes are attached to the same AWG output port. If a multicast has destinations at $l,\ 2 \leq l \leq D$, AWG output ports, then l packet copies are generated and one each is placed in the corresponding virtual queue.

To evaluate the number of packet copies required to service a given generated multicast packet, we need to find the number of AWG output ports that have at least one destination node of the packet attached. Towards this end, we model the N nodes attached to the D AWG output ports as an urn containing N balls in D different colors, i.e., there are $S\ (= N/D)$ balls of color $i,\ i = 1, \ldots, D$. Suppose the considered multicast packet has $\gamma,\ 2 \leq \gamma \leq \Gamma$, destinations. To determine the number of packet copy transmissions we draw γ balls (each representing a destination node) from the urn without replacement. (An urn model with replacement which is a simpler, less accurate model of the multicasting is developed in [47]. In Appendix B we examine the differences between the urn models with and without replacement.) We consider the outcome of the drawing without replacement and study formally the following events:

$C_{k_1,\ldots,k_D}$ = "Event that among γ balls drawn without replacement color 1 occurs k_1 times, color 2 occurs k_2 times, ..., color D occurs k_D times with $k_1 + \cdots + k_D = \gamma$".

The probability of this event is given by the polyhypergeometric distribution [48], which can easily be obtained from the hypergeometric distribution [49], as follows

$$P(C_{k_1,\ldots,k_D}) = \frac{\binom{S}{k_1} \cdots \binom{S}{k_D}}{\binom{N}{\gamma}}. \tag{1}$$

The family of events

$$C_{k_1,\ldots,k_D}\ (0 \leq k_i \leq \gamma \wedge S; i = 1, \ldots, D; \sum_{i=1}^{D} k_i = \gamma) \tag{2}$$

forms a complete system of independent events. Thus

$$P\left(\bigcup_{\substack{0 \leq k_i \leq \gamma \wedge S; 1 \leq i \leq D \\ \sum_{i=1}^{D} k_i = \gamma}} \{C_{k_1,\ldots,k_D}\} \right) = \sum_{\substack{0 \leq k_i \leq \gamma \wedge S; 1 \leq i \leq D \\ \sum_{i=1}^{D} k_i = \gamma}} P(C_{k_1,\ldots,k_D}) = 1. \tag{3}$$

Note that we denote $x \wedge y := \min(x, y)$. In our model, the number Δ of required packet copy transmissions corresponds to the number of distinct colors among the γ balls drawn without replacement.

Towards the evaluation of the distribution of Δ, we define the set of color number vectors

$$\begin{aligned} A_\gamma^l &= \{(k_1,\ldots,k_D)\in\{0,\ldots,S\wedge\gamma\}^D \big| \exists k_{i_1},\ldots,k_{i_l}; i_s\in\{1,\ldots,D\}\,, 1\le s\le l \\ &\quad \text{with } k_{i_s}\ge 1 \text{ and } \sum_{s=1}^{l} k_{i_s}=\gamma; k_r=0 \text{ for } r\neq i_s, 1\le r\le D\} \end{aligned} \tag{4}$$

for $1\le l\le D\wedge\gamma$. Intuitively, this is the set of all color number vectors $(k_1,\ldots,k_D)$ such that there are l distinct colors among the drawn γ balls. The probability that the number Δ of required packet copy transmissions for a given multicast packet with γ destinations is l is then given by

$$P(\Delta=l|\gamma) = \sum_{(k_1,\ldots,k_D)\in A_\gamma^l} P(C_{k_1,\ldots,k_D}). \tag{5}$$

Noting that there are $\binom{D}{l}$ ways of choosing l colors out of the D colors (i.e., choosing l destination ports out of all D AWG output ports), we obtain

$$P(\Delta=l|\gamma=n) = \binom{D}{l} \sum_{\substack{1\le k_1,\ldots,k_l\le n\wedge S;\\ \sum_{i=1}^{l} k_i=n}} \frac{\binom{S}{k_1}\cdots\binom{S}{k_l}}{\binom{N}{n}}, \tag{6}$$

which can be readily computed via recursion, as detailed in Appendix A.

Note that we have calculated in (6) the conditional probability of the event that the number of required packet copies is l given that the generated multicast packet has γ destination nodes, i.e.,

$$P(\Delta=l;\gamma \text{ dest. nodes}) = P(\Delta=l|\gamma \text{ dest. nodes})\cdot P(\gamma \text{ dest. nodes})\cdot P(\text{multicast}) \tag{7}$$

with $P(\gamma \text{ dest. nodes})=\frac{1}{\Gamma-1}$ and $P(\text{multicast})=1-u$.

As noted above, a single packet copy is transmitted if either a unicast packet is generated or the generated multicast packet has all $\gamma, 2\le\gamma\le S\wedge\Gamma$, destination nodes attached to the same AWG output port, i.e.,

$$\begin{aligned} P(\Delta=1) &= P(\text{“gen. unicast pkt“}) + P(\text{“gen. multicast pkt has all dest. at one port“}) \\ &= u+\frac{(1-u)}{(\Gamma-1)}\sum_{\gamma=2}^{S\wedge\Gamma} P(\Delta=1|\gamma) \qquad (8) \\ &= u+\frac{(1-u)}{(\Gamma-1)}\sum_{\gamma=2}^{S\wedge\Gamma} \frac{D\binom{S}{\gamma}\binom{S}{0}\cdots\binom{S}{0}}{\binom{N}{\gamma}} \\ &= u+\frac{(1-u)D}{\Gamma-1}\sum_{\gamma=2}^{S\wedge\Gamma} \frac{S!(N-\gamma)!}{(S-\gamma)!N!}. \qquad (9) \end{aligned}$$

The probability that a given generated packet has destinations at $l,\ 2\le l\le D$, AWG output ports, i.e., requires l packet copy transmissions, is

$$P(\Delta=l) = \frac{(1-u)}{\Gamma-1}\sum_{n=2}^{\Gamma} P(\Delta=l|\gamma=n). \tag{10}$$

We obtain the expected number of required packet copy transmissions as

$$\begin{aligned} E(\Delta) &= P(\Delta = 1) + \sum_{l=2}^{D} l P(\Delta = l) \\ &= u + \frac{(1-u)D}{\Gamma - 1} \sum_{\gamma=2}^{S \wedge \Gamma} \frac{S!(N-\gamma)!}{(S-\gamma)!N!} + \sum_{l=2}^{D} \frac{l(1-u)}{\Gamma - 1} \left(\sum_{n=2}^{\Gamma} P(\Delta = l | \gamma = n) \right). \end{aligned} \tag{11}$$

D. Analysis of Throughput

In this section we calculate the different throughput metrics and establish the stability condition for the network. There are N nodes in the network, each independently generating a new packet at the beginning of a frame with probability σ. Each generated packet requires on average $E[\Delta]$ packet copy transmissions. Thus, the network load in terms of packet copy transmissions per frame is $N \cdot \sigma \cdot E[\Delta]$ in the long run average. Recalling that the AWG provides $D \cdot \Lambda$ wavelength channels, each providing one data phase per frame, we note that the network is stable if $N \cdot \sigma \cdot E[\Delta] < D \cdot \Lambda$.

For stable network operation (and negligible packet drop probabilities), the number of generated packets in a frame is equal to the number of completed packet transmissions (including all the required packet copy transmissions) in a frame in steady state. Hence, the multicast throughput is given by

$$Z_M = N \cdot \sigma. \tag{12}$$

Similarly, we obtain for the transmitter throughput in steady state

$$Z_T = N \cdot \sigma \cdot E[\Delta]. \tag{13}$$

The receiver throughput in steady state is given by

$$Z_R = N \cdot \sigma \cdot \left[u + (1-u) \frac{\Gamma + 2}{2} \right], \tag{14}$$

because a given multicast packet with a maximum multicast size of Γ is received on average by $(\Gamma + 2)/2$ nodes.

E. Arrivals to Virtual Queue

In this section we analyze the packet (copy) arrival to a given virtual queue representing a given AWG input-output port pair. That is, we study the arrivals to one (arbitrary) of the D virtual queues illustrated in Fig. 7.

There are $S = N/D$ nodes attached to the considered AWG input port. Each of the S nodes generates traffic mutually independently of the other nodes. Recall that a given node generates a new unicast data packet with probability $\sigma_u = \sigma \cdot u$ at the beginning of a given frame. With probability $1/D$ that packet is destined to the considered virtual queue.

Next, recall that a given node generates a new multicast packet with probability $\sigma_m = \sigma \cdot (1-u)$ at the beginning of a frame. The number of destination nodes γ is uniformly distributed over $(2, \Gamma)$ and

the individual destination nodes are uniformly distributed over the network nodes, (and consequently AWG output ports and thus virtual queues). Given a multicast packet with γ destination nodes, we need to evaluate the probability that a packet copy is placed in the considered virtual queue. To evaluate this probability we consider now a fixed virtual queue, say the queue associated AWG output port 1, or equivalently, color 1 in the urn model. The event that the multicast packet has at least one destination at AWG output port 1 corresponds to the events $C_{k_1,\ldots,k_D}$ with $0 < k_1 \leq \gamma \wedge S; 0 \leq k_i \leq \gamma \wedge S$; for $i = 2, \ldots, D$, and $\sum_{i=1}^{D} k_i = \gamma$, in our urn model (1). Thus, the probability that a given multicast packet with γ destinations has at least one destination at the considered AWG output port is

$$
\begin{aligned}
& P(\text{“multicast pkt w. } \gamma \text{ dest. has copy to queue } 1'') \\
&= P\left(C_{k_1,\ldots,k_D}(0 < k_1 \leq \gamma \wedge S; 0 \leq k_i \leq \gamma \wedge S; i = 2, \ldots, D; \sum_{i=1}^{D} k_i = \gamma)\right) \\
&= 1 - P\left(C_{k_1,\ldots,k_D}(k_1 = 0; 0 \leq k_i \leq \gamma \wedge S; i = 2, \ldots, D; \sum_{i=2}^{D} k_i = \gamma)\right) \\
&= 1 - \sum_{\substack{0 \leq k_2,\ldots,k_D \leq \gamma \wedge S \\ \sum_{i=2}^{D} k_i = \gamma}} \frac{\binom{S}{k_2} \cdots \binom{S}{k_D}}{\binom{N}{\gamma}} \qquad (15) \\
&= 1 - \frac{(N-\gamma)!(N-S)!}{(N-\gamma-S)!N!} \sum_{\substack{0 \leq k_2,\ldots,k_D \leq \gamma \wedge S \\ \sum_{i=2}^{D} k_i = \gamma}} \frac{\binom{S}{k_2} \cdots \binom{S}{k_D}}{\binom{N-S}{\gamma}} \qquad (16) \\
&= 1 - \frac{(N-\gamma)!(N-S)!}{(N-\gamma-S)!N!}. \qquad (17)
\end{aligned}
$$

Note that we obtained (17) by noting that the sum in (16) is over a complete set of events. Now considering jointly the possibilities that a generated packet is a unicast packet or a multicast packet, the probability that a given node generates a packet (copy) for the considered queue in a given frame is

$$\sigma_q = \frac{\sigma u}{D} + \frac{\sigma(1-u)}{\Gamma - 1} \sum_{\gamma=2}^{\Gamma} \left(1 - \frac{(N-\gamma)!(N-S)!}{(N-\gamma-S)!N!}\right). \qquad (18)$$

Let A be a random variable denoting the number of packet (copy) arrivals to the considered virtual queue in a given frame. Let $a_i = P[A = i]$, $i = 0, 1, \ldots, S$, denote the distribution of A. Clearly with S independent nodes generating traffic for the considered queue,

$$a_i = \binom{S}{i} \cdot \sigma_q^i \cdot (1 - \sigma_q)^{(S-i)}, \qquad (19)$$

for $0 \leq i \leq S$ and $a_i = 0$ for $i > S$. We remark that the average number of packet copies generated by the S nodes attached to a given AWG input port in a frame equals the average number of packet copies arriving to the D virtual queues connecting the input port to the D AWG output ports in a frame, i.e., $S \cdot \sigma \cdot E[\Delta] = S \cdot \sigma_q \cdot D$, which gives a convenient alternative expression for $E[\Delta]$.

F. Queuing Analysis of Virtual Queue

In this section we conduct a queueing analysis of the virtual queue to determine the expected queue length and subsequently the different delay metrics. We begin our formulation by first noting that the arrival process is independent from the state of the queue. Second, we note that the arrival process in frame $t+1$ denoted by A_{t+1} is independent of the arrival process A_t in the prior frame t. Let X_t denote the number of packet (copies) in the queue at the beginning of a given frame t before the new packets are generated for the frame. We impose a maximum virtual queue occupancy J for calculation convenience and set it so large that boundary effects are negligible, i.e., the occupancy J is not reached for stable operation. In each frame up to R packets are served, i.e., $X_{t+1} = \min[(X_t + A_t - R)^+,\ J]$, where $(x)^+ = \max(0, x)$. Thus, $(X_t)_{t\geq 0}$ is a Markov chain with state space $\mathcal{E} := \{\prime, \infty, \ldots, \mathcal{J}\}$ and the following transition matrix $\mathbf{P} = (\mathbf{p}(\mathbf{x}, \mathbf{y}))_{\mathbf{x},\mathbf{y}\in\mathcal{E}}$ with

$$p(x,0) = \begin{cases} \sum\limits_{i=0}^{R-x} a_i \text{ , for } x \leq R \\ 0 \text{ , for } R < x \leq J \end{cases} \tag{20}$$

and

$$p(x,y) = \begin{cases} a_{R+y-x} \text{ , for } x \leq R+y \\ 0 \text{ , for } x > R+y \end{cases} \tag{21}$$

for $0 < y \leq J-1$ and

$$p(x,J) = P(A \geq R + J - x) = \sum_{i=R+J-x}^{N} a_i. \tag{22}$$

From (20)–(22) it follows that $\mathbf{P}$ is an aperiodic and irreducible transition matrix, hence the Markov chain has an unique stationary probability distribution $\pi = [\pi_{\mathbf{0}}, \pi_{\mathbf{1}}, \ldots, \pi_{\mathbf{J}}]$ on $\mathcal{E}$ with $\pi = \pi\mathbf{P}$.

The expected queue length $E[X]$ is given by

$$E[X] = \sum_{j=1}^{J} j \cdot \pi_j. \tag{23}$$

We apply Little's theorem to find the mean copy delay

$$W_{TR} = \frac{E[X]}{S \cdot \sigma_q}. \tag{24}$$

To analyze the mean delay W_M we need to consider the longest among the Δ virtual queues that a packet copy is placed in for a given generated packet. This analysis is complicated by the fact that multicasts with multiple packet copies destined to multiple queues in parallel tend to introduce correlations among the D virtual queues associated with a given AWG input port. Whereby, the larger the number of packet copies Δ, the stronger the correlation. If $\Delta = D$ with a high probability then the D virtual queues behave essentially identically.

For the analytical evaluation of W_M we need to note that the queueing model developed in this section considers a given virtual queue in isolation, i.e., independently of the other $D-1$ queues

associated with the considered AWG input port. To evaluate W_M based on the developed queueing model we employ the following heuristic. If Δ is below a threshold $\kappa \cdot D$ ($< D$), then we evaluate the longest queue with the order statistics of Δ independent virtual queues. If Δ is above the threshold $\kappa \cdot D$, then we approximate the longest queue by the length of one given independent virtual queue.

More formally, let $\hat{X}$ be a random variable denoting the number of packet copies in the longest queue that a given multicast feeds into in a given frame in steady state. Let $X_{[\delta]}$ be a random variable denoting the longest among $\Delta = \delta$ (independent) queues in steady state. From order statistics we obtain that approximately

$$P(X_{[\delta]} = j) = \delta \cdot \left[\sum_{l=1}^{j} \pi_l\right]^{\delta-1} \cdot \pi_j. \tag{25}$$

Hence, approximately

$$\begin{aligned} E[\hat{X}] &= \sum_{\delta=1}^{\kappa \cdot D} \left(\sum_{j=1}^{J} j \cdot P(X_{[\delta]} = j) \right) \cdot P(\Delta = \delta) \\ &\quad + E[X] \cdot \sum_{\delta=\kappa \cdot D+1}^{D} P(\Delta = \delta), \end{aligned} \tag{26}$$

where we assume that $\kappa \cdot D$ is an integer. Applying Little's theorem, we obtain the approximate mean multicast delay

$$W_M = \frac{E[\hat{X}]}{S \cdot \sigma_q}. \tag{27}$$

So far we have assumed that the propagation delay in the network is negligible. We now outline how to incorporate propagation delay into our model. We assume that all nodes are equidistant from the central AWG (which can be achieved with fiber delay lines). We let τ denote the one-way end-to-end propagation delay in frames. We assume that the delay incurred for computing the data packet schedule is negligible (if significant, this delay could also be accounted for by τ). In the network with TDMA control packet transmission and infinite scheduling window considered in this section, each packet incurs a delay of τ from its generation until the receipt of the corresponding control packet by all nodes and the successful scheduling of the data packet (copies). During this delay period the data packet needs to be stored in the node (which we account for in the node buffer dimensioning in Section VI) and can not yet be serviced. The data packet (copies) then incur the delays W_M (W_{TR}) calculated above from the time the transmission schedule has been computed until the last (any arbitrary) packet copy commences its transmission. A given data packet copy incurs a transmission delay equal to the duration of the data phase (which we may roughly approximate by one frame) and a propagation delay τ for the propagation to the destination node. Thus, we need to add $2 \cdot \tau + 1$ frames to the queueing delays W_M and W_{TR} calculated above in order to account for the propagation delay.

TABLE I
NETWORK PARAMETERS AND THEIR DEFAULT VALUES

N	# of nodes in network	200
D	degree (# of ports) of AWG	1,2,4,8
R	number of utilized FSRs	1,2,4,8
Λ	$= D \cdot R$, # of wavelengths = # of transceivers in node	8
σ	packet generation probability	
u	fraction of unicast traffic	1, 0, 0.8
$1-u$	fraction of multicast traffic	0, 1, 0.2
Γ	max # of dest. of multicast pkt	5, 15, 50, 200

V. THROUGHPUT-DELAY PERFORMANCE RESULTS

In this section we numerically study the throughput-delay performance of the $FT^{\Lambda} - FR^{\Lambda}$ AWG network for unicast traffic, multicast traffic, as well as a mix of unicast and multicast traffic. Initially, we fix the number of network nodes at $N = 200$ and the number of used wavelengths (transceivers at each node) at $\Lambda = 8$. The network parameters are summarized in Table I. We assume that the propagation delay is negligible. We plot the numerical results from the probabilistic analysis (A), as well as simulation results (S). Each simulation was warmed up for 10^5 frames and terminated when the 99% confidence intervals of all performance metrics are less than 1% of the corresponding sample means.

A. Unicast Traffic

In Fig. 8 we plot the delay as a function of the throughput for different network configurations with $D \cdot R = \Lambda$ for unicast traffic ($u = 1$). In all these cases, the network has $\Lambda = 8$ wavelengths and $\Lambda = 8$ transceivers at each node. Note that the configuration $(D = 1, R = 8)$ is equivalent to a PSC based network. We observe that the $(D = 8, R = 1)$ network has the largest throughput of up to 64 packets per frame. Due to spatial wavelength reuse the total number of channels for the $(D = 8, R = 1)$ network is $D \cdot \Lambda = 64$. The maximum throughputs for the other three network configurations $(D = 4, R = 2)$, $(D = 2, R = 4)$, and $(D = 1, R = 8)$ are 32, 16, and 8 packets per

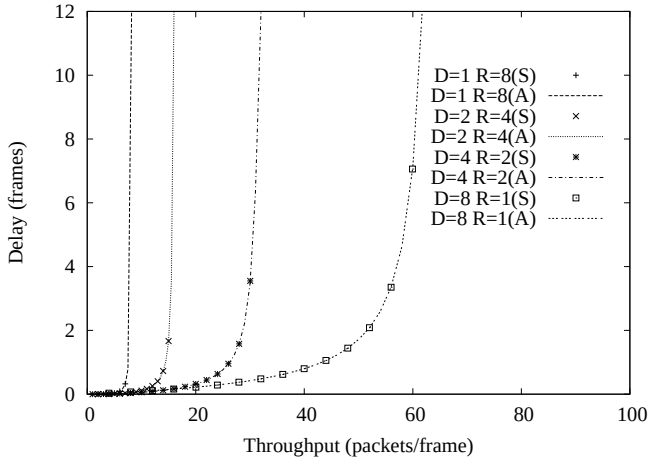

Fig. 8. Delay W_M as a function of throughput Z_M for unicast traffic ($u = 1$).

frame, respectively.

B. Multicast Traffic

In Figures 9 and 10 we plot the throughput and delay for multicast traffic ($u = 0$) for the $(D = 8, R = 1)$ and $(D = 1, R = 8)$ networks for different maximum multicast group sizes Γ. We observe that as Γ increases, both network configurations converge to (i) a maximum multicast

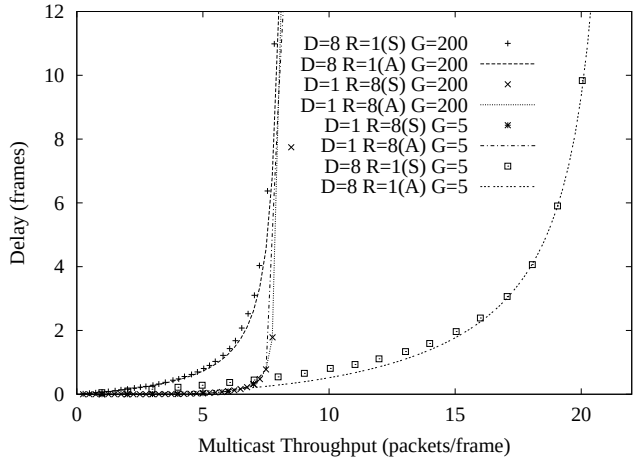

Fig. 9. Delay W_M as a function of multicast throughput Z_M for multicast traffic $(1 - u = 1)$ with $\Gamma = 5$ and $\Gamma = 200$.

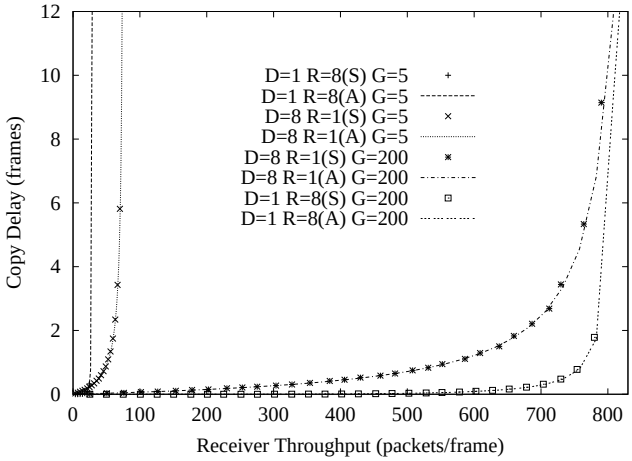

Fig. 10. Copy delay W_{TR} as a function of receiver throughput Z_R for multicast traffic $(u = 0)$ with $\Gamma = 5$ and $\Gamma = 200$.

throughput of 8 packets/frame, and (ii) the maximum receiver throughput of 800 packets/frame. To understand these dynamics consider the transmission of broadcast packets that are destined to all $N = 200$ receivers in both networks. Clearly, in the PSC equivalent $(D = 1, R = 8)$ network at most eight packet transmissions can take place simultaneously, each reaching all 200 receivers. In the $(D = 8, R = 1)$ network, the broadcast of one packet requires the transmission of eight packet copies, one to each AWG output port, and reaching $N/D = 25$ receivers. Thus in both networks the multicast throughput, i.e., the number of completed multicasts per frame, is 8 packets/frame and the receiver throughput is 1600 packets/frame. Note that in this broadcast scenario the transmitter throughput is 8 packets/frame in the $(D = 1, R = 8)$ network and 64 packets/frame in the $(D = 8, R = 1)$ network.

Now with multicast traffic with a maximum multicast group size of $\Gamma = 200$, a multicast packet has on average 100 destination nodes. The probability that at least one of these destination node is attached to each AWG output port is $P(\Delta = D|\gamma = 100) = 0.98$. Thus it is very likely that D copies of the multicast packet need to be transmitted. In general, when multicasting over the $FT^{\Lambda} - FR^{\Lambda}$ AWG network, there are two effects at work. On one hand, a large AWG degree D increases the spatial wavelength reuse as all Λ wavelengths can be reused at each AWG port. On the other hand, as the multicast group size increases it becomes (for uniformly distributed destination nodes) increasing likely that at least one destination node is located at each AWG output port. The increase in spatial wavelength reuse in the network configuration with larger D is thus compensated by the increase in the number of required packet copy transmissions when the multicast group size

is large. There is a net effect gain in the throughput performance whenever the number of required copy transmissions is smaller than the spatial reuse factor D, i.e., when the multicast group size is relatively small or when the destination nodes tend to be co-located at a small number of AWG output ports. Indeed, as we see from Fig. 10, for a maximum multicast group size of $\Gamma = 5$ and a copy delay of 2 frames, the $(D = 8, R = 1)$ network achieves roughly twice the receiver throughput of the $(D = 1, R = 8)$ network.

Note that these multicast dynamics with transceiver arrays are fundamentally different from the dynamics with a single tunable transceiver at each node. In the single transceiver network [3], [15], large multicasts are very difficult to schedule as it becomes increasingly unlikely to find the receivers of all destination nodes to be free at the same time, resulting in the so-called receiver bottleneck. Hence it is advantageous to partition multicast groups into several smaller subgroups and transmit copies to each subgroup. The increased number of copy transmissions may lead to a channel bottleneck on the PSC which can be relieved by the increased number of wavelength channels obtained from spatial wavelength reuse on the AWG. The increased number of transmissions on these larger number of channels in turn can exacerbate the receiver bottleneck with single transceiver nodes [3], [15].

Returning to multicasting with transceivers arrays, which overcome the receiver bottleneck, we observe from Figures 9 and 10 that the $(D = 8, R = 1)$ network gives larger delays than the $(D = 1, R = 8)$ network for large multicast group sizes. This is because the multiple packet copy transmissions required for large multicast group sizes in the $(D = 8, R = 1)$ network are more difficult to schedule than the single packet transmission in the $(D = 1, R = 8)$ network.

In summary, we find that the $FT^{\Lambda} - FR^{\Lambda}$ AWG network has significantly improved throughput performance compared with an equivalent PSC network for small multicast groups or co-located multicast destinations. For large multicast groups with uniformly distributed destinations the PSC network achieves smaller delays.

C. Mix of Unicast and Multicast Traffic

In this section we consider mixes of unicast and multicast traffic, which are likely to arise in metropolitan area networks. Throughout this section we fix the maximum multicast size at $\Gamma = 200$. In Fig. 11 we plot the throughput-delay performance of the $FT^{\Lambda} - FR^{\Lambda}$ AWG network for 80% unicast traffic and 20% multicast traffic for different network configurations. For this traffic mix scenario, we consider both the Bernoulli traffic generation described in Section IV-A as well as self-similar traffic generation. In particular, we generate self-similar packet traffic with a Hurst parameter of 0.75, by aggregating ON/OFF processes with Pareto distributed on-duration and geometrically distributed off-duration [50]. We observe that with increasing AWG degree D the network achieves significantly larger multicast throughputs while the delay is increased only very slightly (at lower throughput levels). The throughput levels of the $(D = 8, R = 1)$ configuration are approximately three times larger than for the PSC equivalent $(D = 1, R = 8)$ configuration.

This performance improvement is due to the increased spatial wavelength reuse with increased D, which is only to a small degree compensated for by the increased number of multicast packet copy transmission for that typical mixed traffic scenario. In the PSC based network $(D = 1)$ each

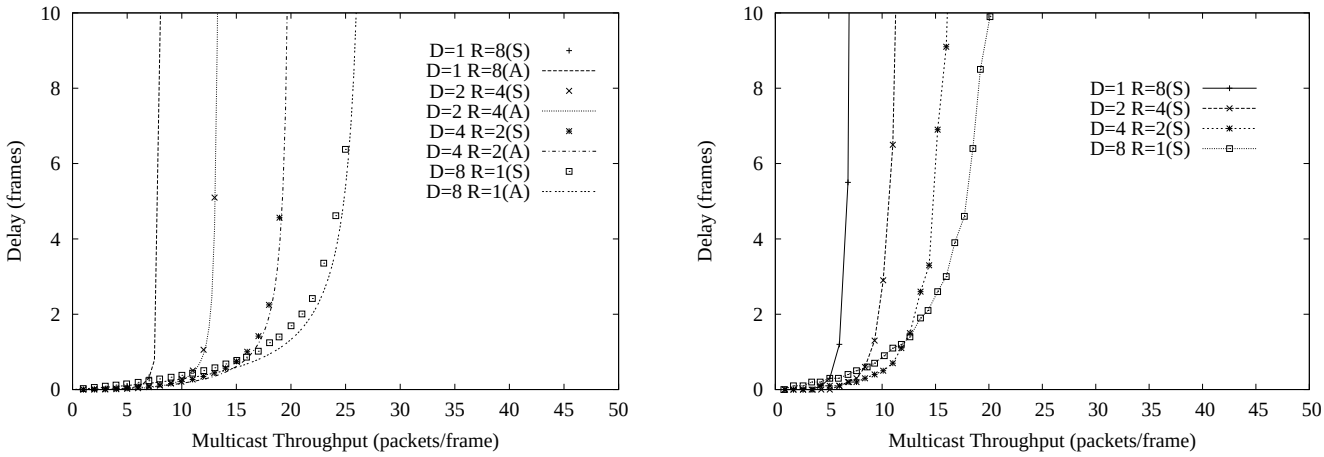

(a) Bernoulli traffic (b) Self-similar traffic

Fig. 11. Delay W_M as a function of multicast throughput Z_M for mix of 80% unicast ($u = 0.8$) and 20% multicast traffic with $\Gamma = 200$.

packet transmission occupies one of the Λ wavelength channels irrespective of whether the packet is a unicast or a multicast packet. In the AWG based network ($D \geq 2$), each of the Λ wavelength channels can be reused at each AWG port, i.e., D times, and additional copy transmissions are only required when the destination nodes of a given packet are attached to multiple AWG output ports. Thus, a larger AWG degree is overall beneficial when a significant portion of the traffic is unicast traffic.

We also observe from Fig. 11 that for self-similar traffic, the packet delays are somewhat larger compared to the delays for Bernoulli traffic. This is because with self-similar traffic generation, the packets arrive typically in bursts, which result in larger backlogs and longer queuing delays for the packets making up the tail end of a burst. (The impact of the self-similar traffic on the buffer requirements is studied in Section VI.) Nevertheless, the overall performance trends, i.e., generally larger throughput and slightly increased delay at low throughput levels for larger D, are very similar both for Bernoulli and self-similar traffic. Hence, we focus on Bernoulli traffic for the remainder of this section.

In Figures 12 and 13, we plot the receiver throughput-delay performance for 60% and 90% unicast traffic. Note that the multicast throughput of the $(D = 1, R = 8)$ network is limited to at most 8 packets/frame. We observe that the gap in performance between the PSC based network ($D = 1, R = 8$) and the AWG based network with $D = 8$ widens as the fraction of unicast traffic increases. For 90% unicast traffic the $(D = 8, R = 1)$ network achieves about three times the throughput of the $(D = 1, R = 8)$ network; although the receiver throughput level is overall reduced for the larger portion of unicast traffic. Again we observe that the increase in throughput comes at the expense of only a minor increase in delay (nicely visible in Fig. 13 for the $u = 0.6$ scenario in the throughput range from $100 - 280$ packets/frame).

We observe that the accuracy of our probabilistic analysis is overall quite good. The discrepancies between the analytical and simulation results for the delay W_M for larger D are primarily due to the heuristic approximation (26) of the occupancy distribution of the longest queue, for which we set $\kappa = 0.75$ throughout this paper.

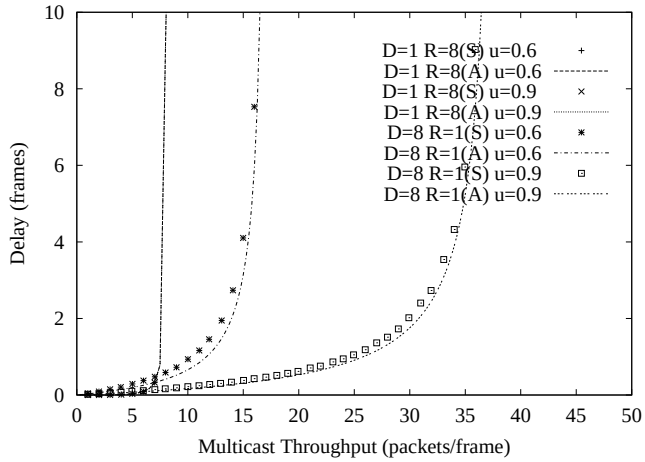

Fig. 12. Delay W_M as a function of multicast throughput Z_M for mixed traffic $u = 0.9$ and $u = 0.6$.

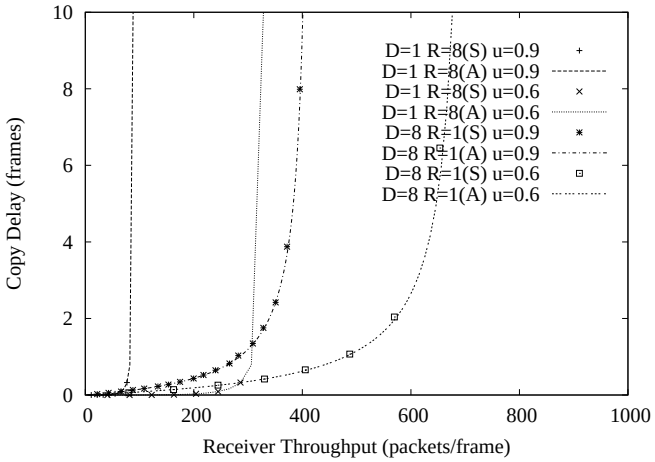

Fig. 13. Copy delay W_{TR} as a function of receiver throughput Z_R for mixed traffic $u = 0.9$ and $u = 0.6$.

TABLE II

THROUGHPUT (IN PACKETS/FRAME) AND DELAY (IN FRAMES) FOR $(D = 1, R = 8)$ NETWORK FOR MIXED TRAFFIC $(u = 0.8)$ WITH $\Gamma = 200$

σ	Z_M	Z_T	Z_R	W_M	W_{TR}
0.01	2.0	2.0	41.8.0	0.0	0.0
0.02	4.0	4.0	83.7	0.01	0.01
0.035	7.0	7.0	146.5	0.33	0.33
0.040	0.79	8.0	167.5	45.4	45.4

TABLE III

THROUGHPUT (IN PACKETS/FRAME) AND DELAY (IN FRAMES) FOR $(D = 8, R = 1)$ NETWORK FOR MIXED TRAFFIC $(u = 0.8)$ WITH $\Gamma = 200$

σ	Z_M	Z_T	Z_R	W_M	W_{TR}
0.01	2.0	4.6	38.6	0.06	0.04
0.02	4.0	9.4	79.7	0.12	0.08
0.04	8.0	18.8	160.4	0.28	0.21
0.08	15.9	37.4	319.8	0.86	0.67
0.125	25.0	58.7	501.9	6.38	5.28
0.135	27.0	63.9	549.0	150.5	127.3

Tables II and III show the detailed throughput-delay performance metrics obtained from simulation for the scenario with 80% unicast and 20% multicast traffic for the $(D = 1, R = 8)$ and $(D = 8, R = 1)$ network configurations. The stability limit (capacity) for the $(D = 8, R = 1)$ network is $D \cdot \Lambda = 64$ packets per frame. We observe from Table III that for a packet generation probability σ of 0.08 and less, corresponding to a transmitter throughput Z_T of 37.4 or less, or equivalently less than 58% of the capacity, the delays are very small. As the load increases to 90% of the capacity and higher, the delays become quite large. We also observe from Table III that for the $(D = 8, R = 1)$ network the average copy delay W_{TR} is for lower loads typically 75% or less of the corresponding delay W_M for completing the transmission of all packet copies.

In Tables IV and V we summarize the results of the network performance for the various AWG configurations for different traffic conditions. The data entries are extrapolated from our simulation results. In Table IV we fix the delay at 4 frames and record the maximum multicast throughput. In Table V we fix the copy delay at 4 frames and record the maximum receiver throughput. We observe that both in terms of multicast throughput and receiver throughput, the $(D = 8, R = 1)$ network outperforms the networks with small D. In general, the performance of the network improves as D becomes larger. This demonstrates the advantages of the spatial wavelength reuse of the AWG. The performance gap narrows for multicast-only traffic as the average number of destination nodes

TABLE IV
MULTICAST THROUGHPUT Z_M (IN PACKETS/FRAME) FOR DELAY W_M OF 4 FRAMES

(D,R)	$(u=1)$	$(u=0)$ $\Gamma=5$	$(u=0)$ $\Gamma=15$	$(u=0)$ $\Gamma=200$	$(u=0.8)$ $\Gamma=200$
$(1,8)$	7.9	7.9	7.9	7.9	7.9
$(2,4)$	15.8	9.4	8.1	7.6	12.6
$(4,2)$	31.2	12.3	8.4	7.4	19.7
$(8,1)$	60.4	18.7	9.2	7.1	26.9

TABLE V
RECEIVER THROUGHPUT Z_R (IN PACKETS/FRAME) FOR COPY DELAY W_{TR} OF 4 FRAMES

(D,R)	$(u=1)$	$(u=0)$ $\Gamma=5$	$(u=0)$ $\Gamma=15$	$(u=0)$ $\Gamma=200$	$(u=0.8)$ $\Gamma=200$
$(1,8)$	8	27	62	785	160
$(2,4)$	16	30	66	762	245
$(4,2)$	31	41	73	750	397
$(8,1)$	60	64	97	730	490

increases, and for the $u = 0$, $\Gamma = 200$ scenario the $(D = 1, R = 8)$ network gives the largest throughputs. However, for mixed unicast and multicast traffic, both the multicast throughput and the receiver throughput improves significantly as D increases. Both the multicast throughput and the receiver throughput for the $(D = 8, R = 1)$ configuration are over 3 times that of the $(D = 1, R = 8)$ PSC network.

D. Impact of Number of Transceivers

In this section we study the throughput-delay performance of the $FT^{\Lambda} - FR^{\Lambda}$ AWG network for different numbers of transceivers Λ in each node. Throughout this section we fix the number of network nodes at $N = 200$ and the number of used FSRs at $R = 1$, hence $D = \Lambda$. Recall from Section II that the length of the control phase is N/Λ slots, each carrying one control packet. For our numerical evaluations in this and the following sections we consider a control packet length of 2 bytes and a data packet length of 1500 bytes. Thus the length of the control phase varies between 200 slots for (the degenerate case of) $\Lambda = 1$ and 25 slots for $\Lambda = 8$. The corresponding frame length varies between 950 slots and 775 slots. In Fig. 14 we plot the throughput-delay performance for the different Λ $(= D)$. The delay is given in slots and the throughput is given in steady state, i.e., normalized by the ratio of data phase to total frame length. We observe that the throughput

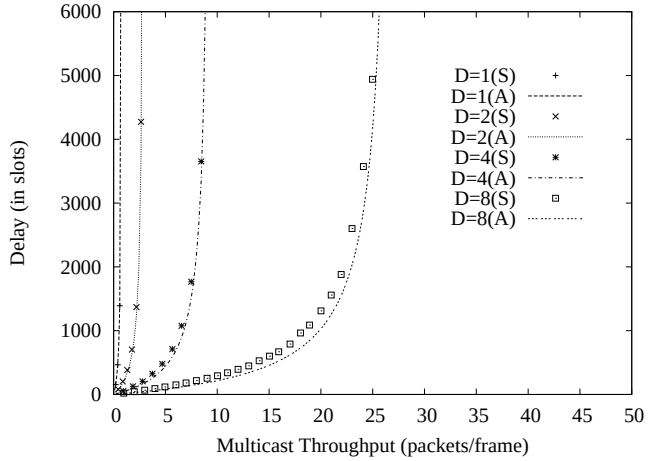

Fig. 14. Delay W_M as a function of multicast throughput Z_M for mix of 80% unicast $(u = 0.8)$ and 20% multicast traffic with $\Gamma = 200$ for different number of transceivers Λ $(= D)$

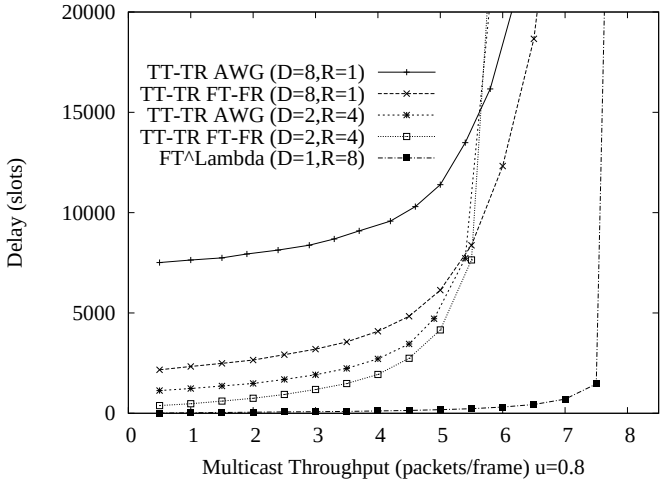

Fig. 15. Delay W_M as a function of multicast throughput Z_M for TT–TR AWG, TT–TR–FT–FR AWG, and $FT^{\Lambda} - FR^{\Lambda}$ AWG networks

for a fixed tolerable delay approximately triples as the number of nodal transceivers Λ doubles.

There are two main effects at work here. On the one hand, the doubled number Λ of transceivers and the doubled wavelength reuse (governed by $D = \Lambda$) together quadruple the network capacity $D \cdot \Lambda$ (maximum number of data packet (copy) transmissions per frame). On the other hand, the increased number of required packet copy transmissions (for the larger D) results in increased delay. Overall, we observe that large throughputs are achieved for small numbers of transceivers Λ due to the extensive wavelength reuse on the AWG.

E. Comparison between TT–TR AWG Network and $FT^{\Lambda} - FR^{\Lambda}$ AWG Network

In this section we compare the throughput-delay performance of the $FT^{\Lambda} - FR^{\Lambda}$ AWG network with the TT–TR AWG network employing one tunable transceiver at each node. Specifically, we consider (*i*) a TT–TR AWG network where the control packets are transmitted with an LED (as in [2], [3]) over the AWG, and (*ii*) a TT–TR–FT–FR AWG network where the control packets are transmitted over a PSC with a separate FT–FR at each node and the wavelengths on the AWG are available for data transmission all the time. TDMA control packet transmission is employed in all networks. We employ greedy data packet scheduling in the TT–TR AWG networks, which schedules a data packet for transmission to an AWG output port if at least one of the intended receivers at the port is free. This may result in multiple transmissions of a given multicast packet to a given AWG output port. This greedy policy is a reasonable benchmark for our comparisons as it tends to alleviate the receiver bottleneck at the expense of an increased burden on the transmitters, which as we demonstrate in the next section is a reasonable strategy.

In Figure 15, we plot the throughput-delay performances of the two types of TT–TR AWG networks for different (D, R) combinations and compare with the $(D = 1, R = 8)$ $FT^{\Lambda} - FR^{\Lambda}$ AWG network, which gives the worst throughput-delay performance of all (D, R) combinations for the $FT^{\Lambda} - FR^{\Lambda}$ AWG network, see Fig. 11. We observe that all configurations of the TT–TR–FT–FR AWG network, which represents the best possible performance of a TT–TR AWG network in that all control is conducted in parallel over the PSC, has significantly lower performance than the worst performing $FT^{\Lambda} - FR^{\Lambda}$ AWG network configuration. The large delays for the TT–TR AWG network are due to the LED control packet transmission which is conducted in cycles of length D frames [2], [3].

F. Transceiver Utilization

In this section we study the utilization of the transmitters and receivers in the $FT^{\Lambda} - FR^{\Lambda}$ and TT–TR AWG networks We define the transmitter utilization U_T as the average fraction of time that any given transmitter is busy transmitting data packets in steady state. For the $FT^{\Lambda} - FR^{\Lambda}$ AWG network, clearly $U_T = Z_T/(N \cdot \Lambda) = \sigma \cdot E[\Delta]/\Lambda$. We define the receiver utilization U_R as the average fraction of time that any given receiver is busy receiving data packets in steady state. For the $FT^{\Lambda} - FR^{\Lambda}$ AWG network, clearly $U_R = Z_R/(N \cdot \Lambda) = \sigma \cdot [u + (1 - u) \cdot (\Gamma + 2)/2]/\Lambda$.

For the TT–TR AWG network, the transmitter utilization is difficult to compute because with the employed greedy scheduling algorithm, a packet copy destined to multiple receivers attached to the same splitter can be transmitted multiple times depending on receiver availability. The receiver utilization for the TT–TR AWG network is approximately equal to the average number of

TABLE VI
TRANSCEIVER UTILIZATION COMPARISON FOR MIXED TRAFFIC ($u = 0.8$) WITH $\Gamma = 200$ FOR DELAY OF 10,000 SLOTS

AWG Network	Z_T	U_T	Z_R	U_R
FT–FR–TT–TR ($D = 8, R = 1$)	22	0.11	126	0.63
FT^{Λ} ($D = \Lambda = 1$)	0.7	0.003	15	0.08
FT^{Λ} ($D = \Lambda = 2$)	3.6	0.01	60	0.15
FT^{Λ} ($D = \Lambda = 4$)	15	0.02	191	0.24
FT^{Λ} ($D = \Lambda = 8$)	61	0.04	535	0.33

destinations per packet multiplied by the packet throughput, i.e., $U_R = \sigma \cdot [u + (1 - u) \cdot (\Gamma + 2)/2]$.

In Table VI we compare the average transceiver utilization of the TT–TR–FT–FR AWG and the $FT^{\Lambda} - FR^{\Lambda}$ AWG networks for traffic loads resulting in an average delay of 10,000 slots. We observe that for the considered traffic mix with 80% unicast traffic and 20% multicast traffic, the utilization of the fixed tuned transmitters in the $FT^{\Lambda} - FR^{\Lambda}$ AWG network is below 4% for all considered configurations. On the other hand, the fixed tuned receivers are fairly well utilized, especially for the configurations with larger D. This suggests to study $TT^{i} - FR^{\Lambda}$ AWG networks, with $1 \leq i < \Lambda$ in future work. This is further indicated by the utilization of approximately 11 % of the tunable transmitter in the TT–TR–FT–FR AWG network. The tunable receiver in the TT–TR–FT–FR AWG network is heavily utilized, which illustrates the receiver bottleneck in TT–TR AWG networks and also indicates that an array of fixed tuned receivers is a good choice for an AWG based metro network carrying mixed traffic.

G. Control Packet Transmission: TDMA vs. Contention

In this section we examine the impact of the TDMA and contention based control packet transmission strategies described in Sections III-A and III-B. We consider the $FT^{\Lambda} - FR^{\Lambda}$ AWG network with $D = 4$, $R = 2$, and $\Lambda = 8$ for a mix of 80% unicast ($u = 0.8$) and 20% multicast traffic with $\Gamma = 200$. The length of the data phase is fixed at 1500 bytes or equivalently 750 slots throughout. In Fig. 16 we compare the throughput-delay obtained from simulation for (i) TDMA control packet transmission with a control phase with N/Λ slots, and (ii) control packet transmission with contention with a control phase with $M = 5$ and 10 slots. We observe from Fig. 16a) that for $N = 200$ nodes, TDMA control packet transmission gives better throughput delay performance than control packet contention. This is because the effect of the slightly shorter control phase with contention is outweighed by the delay introduced due to control packet collisions and subsequent retransmissions. Note that each retransmission introduces an additional delay of one frame, whereby in the considered scenario the frame is significantly longer than the control phase.

Control packet transmission with contention is advantageous when the length N/Λ of the TDMA control phase makes up a significant portion of the frame length, i.e., when either the number of nodes N is large or the data packets are short. We illustrate this effect by scaling up the number of nodes to $N = 2000$ in Fig. 16b). We observe that in this scenario, control packet contention with a data phase consisting of $M = 10$ slots gives consistently better throughput-delay performance than TDMA control packet transmission. This is because in this scenario, the effect of the significantly

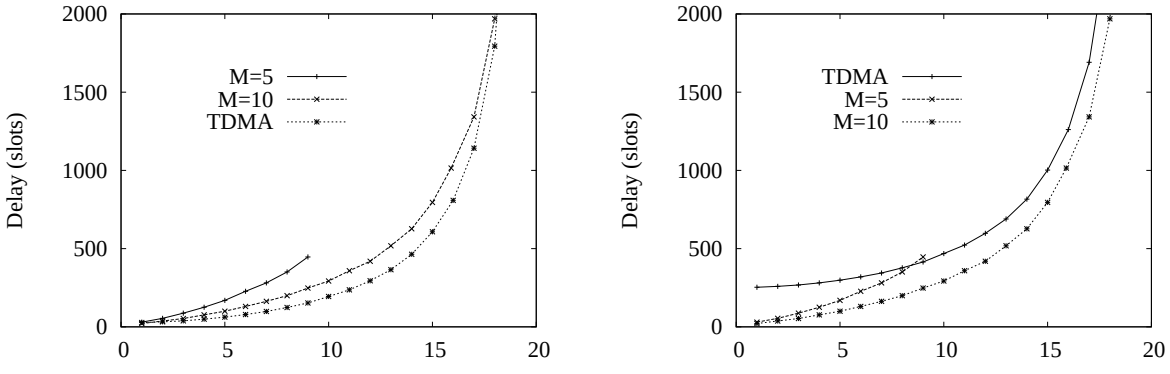

Fig. 16. Delay W_M in slots as a function of multicast throughput Z_M for control packet transmission with TDMA (N/Λ slot control phase) and contention (M slot control phase)

shorter control phase with contention outweighs the effect of occasional control packet collisions and retransmissions. If the number of control slots is too small, then the control packet contention becomes increasingly a bottleneck as the traffic load increases, as illustrated in Fig. 16b) for $M = 5$.

VI. Node Buffer Dimensioning

In this section we address the problem of dimensioning the buffer in a node. Note that the analysis in Section IV considered virtual queues, whereby a virtual queue buffers the packet (copies) originating from the nodes attached to a given AWG input port and destined to nodes at a given AWG output port. We introduced the virtual queue as a modelling concept to make the above analysis tractable. In a real network the packets are buffered in node buffers. The dimensioning of these node buffers is important for network dimensioning and resource allocation. The probabilistic modelling of the nodal buffer occupancy is a complex problem due to the sharing of the wavelengths connecting a given AWG input-output port pair among the nodes connected to the input port and the multiple packet copies required to serve a multicast packet and is left for future work.

We conduct simulations of the $FT^{\Lambda} - FR^{\Lambda}$ network with the buffering at the nodes to determine the packet drop probability P_{loss} which we define as the probability that a newly generated packet finds the nodal buffer full and is dropped. We denote L for the buffer capacity in number of data packets at each node, whereby only one copy of each data packet is stored irrespective of the number of packet copy transmissions required to serve the packet. We consider the network with the default parameters given in Table I for a mix of 80% unicast traffic ($u = 0.8$) and 20% multicast traffic with $\Gamma = 200$. We consider both a network with a negligible propagation delay $\tau = 0$ and a network with a propagation delay of $\tau = 94$ frames, which corresponds to a typical scenario with a distance of 48.6 km between a node and the central AWG, a propagation speed of $2 \cdot 10^8$ m/sec, a frame length of 1550 bytes, and an OC48 transmission rate of 2.4 Gbps. Also, we consider both Bernoulli (denoted `ber`) and self-similar (denoted `ssim`) traffic generation. In Fig. 17 we plot the packet drop probability P_{loss} at a node as a function of the probability σ that a node generates a new packet in a frame. We observe that for Bernoulli traffic and a negligible propagation delay, relatively small

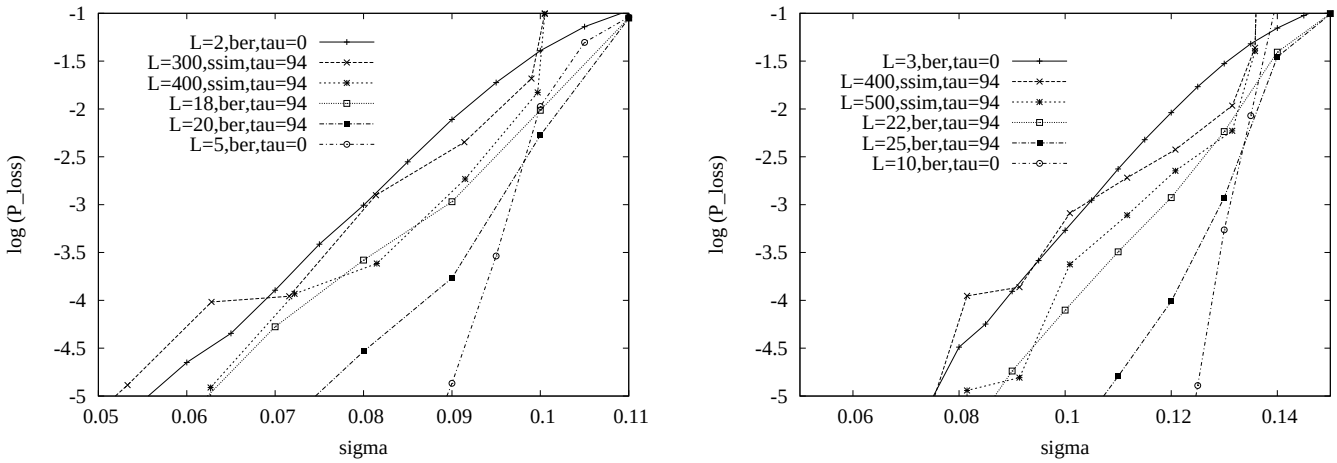

(a) $D = 4$ AWG ports and $R = 2$ FSRs (b) $D = 8$ AWG ports and $R = 1$ FSRs

Fig. 17. Packet drop probability P_{loss} at node as a function of packet generation probability σ at node for different node buffer capacities L in packets.

node buffers with a capacity of 5 or 10 data packets are sufficient to achieve small loss probabilities on the order of 10^{-2} or less for traffic loads close to the stability limit of the networks. Recall from Section IV-D that the stability limit for the network is $\sigma < D \cdot \Lambda/(N \cdot E[\Delta])$, which is $\sigma < 0.1$ for the considered $D = 4$, $R = 2$ network and $\sigma < 0.14$ for the considered $D = 8$, $R = 1$ network. For a propagation delay of $\tau = 94$ frames, correspondingly larger buffers are needed to store the data packets for which the control packets are propagating through the network. For self-similar traffic and a propagation delay of $\tau = 94$ frames, yet larger buffers are required to ensure small packet drop probabilities. We observe from Fig. 17(b), however, that a buffer capable of holding 500 data packets (= 750 kbyte for the considered 1500 byte data packets) is sufficient to ensure loss probabilities below $10^{-3.5}$ for a long run mean packet generation probability of $\sigma = 0.1$ (which for the considered network parameters corresponds to a long run average traffic generation rate of 232 Mbps of the bursty self-similar traffic with Hurst parameter $H = 0.75$).

VII. Conclusion

In this paper we have developed and evaluated the $FT^{\Lambda} - FR^{\Lambda}$ AWG network, an AWG based single-hop metro WDM network with a fixed-tuned transceiver based node architecture. All building blocks of the network are well-understood and commercially available, making the network practical and readily deployable. Our analytical and simulation results indicate that the $FT^{\Lambda} - FR^{\Lambda}$ AWG network efficiently supports a typical mix of unicast and multicast traffic. For such a traffic mix the $FT^{\Lambda} - FR^{\Lambda}$ AWG network with an 8×8 AWG achieves about three times the throughput of an equivalent PSC based network.

There are several avenues for future work. One direction for future work is motivated by the finding in this paper that for a typical mix of unicast and multicast traffic, the utilization of the Λ fixed tuned transmitters in the $FT^{\Lambda} - FR^{\Lambda}$ AWG network is relatively low, while the Λ fixed tuned receivers are relatively highly utilized. This finding suggests to study AWG based networks employing fast tunable transmitters and arrays of fixed tuned receivers. Such $FT^{i} - FR^{\Lambda}$ AWG networks with $1 \leq i < \Lambda$ appear also attractive from a technological perspective as fast tunable

transmitters are currently a relatively more mature technology compared to fast tunable optical filter receivers.

Another important direction for future work is to study efficient protection strategies for the AWG based star networks.

Appendix A: Evaluation of $P(\Delta = l|\gamma = n)$

In this appendix, we detail how to evaluate $P(\Delta = l|\gamma = n)$ given by (6). For $l = 2$, (6) takes the form

$$P(\Delta = 2|\gamma = n) = \binom{D}{2} \sum_{\substack{1\le k_1,k_2\le n\wedge S \\ k_1+k_2=n}} \frac{\binom{S}{k_1}\binom{S}{k_2}}{\binom{N}{n}} \tag{28}$$

$$= \binom{D}{2} \sum_{k_1=\max(1,n-S)}^{\min(n-1,S)} \frac{\binom{S}{k_1}\binom{S}{n-k_1}}{\binom{N}{n}}. \tag{29}$$

We define Q to represent the sum in (29), i.e.,

$$Q(\Delta = 2|\gamma = n) = \sum_{k_1=\max(1,n-S)}^{\min(n-1,S)} \binom{S}{k_1}\binom{S}{n-k_1}. \tag{30}$$

We note that when l increases by one in (6), we are adding one more term $\binom{S}{k_l}$. Thus

$$Q(\Delta = 3|\gamma = n) = \sum_{\substack{1\le k_1,k_2,k_3\le n\wedge S \\ k_1+k_2+k_3=n}} \binom{S}{k_1}\binom{S}{k_2}\binom{S}{k_3} \tag{31}$$

$$= \sum_{k_3=\max(1,n-2S)}^{\min(n-2,S)} Q(\Delta = 2|\gamma = n-k_3)\binom{S}{k_3}. \tag{32}$$

In general,

$$Q(\Delta = l|\gamma = n) = \sum_{k_l=\max(1,n-(l-1)S)}^{\min(n-l+1,S)} Q(\Delta = l-1|\gamma = n-k_l)\binom{S}{k_l}. \tag{33}$$

With the $Q(\Delta = l|\gamma = n)$, we can easily compute

$$P(\Delta = l|\gamma = n) = \binom{D}{l} \cdot \frac{Q(\Delta = l|\gamma = n)}{\binom{N}{n}}. \tag{34}$$

Appendix B: Comparison of Urn Models With and Without Replacement for Multicasting

In this appendix we compare the urn model with replacement for the multicasting developed in [47] with the urn model without replacement developed in this paper. The urn model with replacement is simpler as it does not keep track of the balls that have already been drawn. Instead, when a ball (node) is drawn, the color (AWG output port) of the ball is noted, and the ball is put

TABLE VII

PROBABILITY DISTRIBUTION AND EXPECTED VALUE OF NUMBER OF AWG OUTPUT PORTS WITH MULTICAST DESTINATIONS FOR $N = 20$ NODE NETWORK WITH $D = 4$ AND $S = 5$ FOR MULTICAST TRAFFIC ($u = 0.0$) WITH $\Gamma = 10$

	$P(\Delta = 1)$	$P(\Delta = 2)$	$P(\Delta = 3)$	$P(\Delta = 4)$	$E[\Delta]$
Urn with Repl.	0.037	0.222	0.371	0.371	3.075
Urn w/o Repl.	0.028	0.189	0.310	0.473	3.228
Simulation	0.027	0.190	0.309	0.473	3.228

back into the urn. Then the next ball is drawn, and so on. This urn model with replacement makes a modelling error in that it allows a given node to be drawn multiple times as a destination of a given multicast. In contrast, the urn model without replacement allows each node to be counted only once as a destination of a given multicast. To illustrate these effects, consider a network with $D = 2$ AWG input ports and $D = 2$ output ports, $N = 2$ nodes and $S = 1$ nodes attached to each AWG output port for multicast traffic ($u = 0$) destined to two nodes ($\gamma = 2$). Clearly, in this scenario, each packet is destined to both AWG output ports, i.e., $P(\Delta = 2|\gamma = 2) = 1$, as correctly modelled by the urn model without replacement. With the urn model with replacement, on the other hand, we obtain $P(\Delta = 1|\gamma = 2) = 0.5$ and $P(\Delta = 2|\gamma = 2) = 0.5$. To see this, note that with probability 0.5 the ball selected in the second drawing is identical to the ball selected in the first drawing, with probability 0.5 the other ball is selected.

The modelling error of the urn model with replacement decreases as the probability of drawing the same ball multiple times decreases, which decreases as the number of balls (nodes in the network) increases. To illustrate the effect of the decreasing modelling error, we compare in Table VII the probability distribution and expected value of the number of AWG output ports with attached destination nodes obtained from the urn model with replacement, the urn model without replacement, and simulations for a network with $N = 20$ nodes with $D = 4$ and $S = 5$ for multicast traffic $u = 0$ with a maximum of $\Gamma = 10$ destination nodes. We observe from the table that the urn model with replacement gives too large values for the probabilities that the destinations are attached to a small number of AWG output ports and too small values for the probability that the multicast destinations are attached to a large number of AWG output ports. The urn model with replacement gives thus overall too small values for the expected number of AWG output ports with multicast destinations $E[\Delta]$. For the considered $N = 20$ node network, the urn model with replacement underestimates $E[\Delta]$ by almost 5%, which results in a correspondingly large underestimation of the transmitter throughput Z_T (13), the probability of generating a packet copy for a virtual queue σ_q (18), and the delays. We also observe from the table that the results obtained with the urn model with replacement closely match the simulation results.

In Table VIII, we consider a $N = 200$ node network with $D = 8$ and $S = 25$ for a mix of 80% unicast traffic ($u = 0.8$) and 20% multicast traffic with $\Gamma = 200$. We observe from the table that the results from both urn models match the simulation results very closely. This is due to (i) the large fraction of unicast traffic for which the modelling error of selecting the same ball multiple times does not arise, and (ii) the large number of network nodes, which results in a small probability of

TABLE VIII

PROBABILITY DISTRIBUTION AND EXPECTED VALUE FOR NUMBER OF AWG OUTPUT PORTS WITH MULTICAST DESTINATIONS FOR $N = 200$ NODE NETWORK WITH $D = 8$ AND $S = 25$ FOR MIX OF 80% UNICAST TRAFFIC ($u = 0.8$) AND 20 % MULTICAST TRAFFIC WITH $\Gamma = 200$

	$P(\Delta = 1)$	$P(\Delta = 2)$	$P(\Delta = 3)$	$P(\Delta = 4)$	$P(\Delta = 5)$	$P(\Delta = 6)$	$P(\Delta = 7)$	$P(\Delta = 8)$	$E[\Delta]$
Replacement	0.800	0.001	0.002	0.002	0.003	0.004	0.008	0.180	2.351
Refined	0.800	0.001	0.002	0.002	0.003	0.004	0.007	0.181	2.353
Simulation	0.800	0.001	0.001	0.002	0.003	0.004	0.007	0.183	2.364

selecting the same ball multiple times in the urn model with replacement.

ACKNOWLEDGMENT

We are grateful to Martin Maier for insightful discussions during the early stages of this research.

REFERENCES

[1] B. Mukherjee, "WDM optical communication networks: Progress and challenges," *IEEE Journal on Selected Areas in Communications*, vol. 18, no. 10, pp. 1810–1824, Oct. 2000.

[2] M. Scheutzow, M. Maier, M. Reisslein, and A. Wolisz, "Wavelength reuse for efficient packet-switched transport in an AWG-based metro WDM network," *IEEE/OSA Journal of Lightwave Technology*, vol. 21, no. 6, pp. 1435–1455, June 2003.

[3] M. Maier, M. Scheutzow, and M. Reisslein, "The arrayed–waveguide grating based single–hop WDM network: an architecture for efficient multicasting," *IEEE Journal on Selected Areas in Communications*, vol. 21, no. 9, pp. 1414–1432, Nov. 2003.

[4] K. V. Shrikhande, I. M. White, M. Rogge, F.-T. An, A. Srivatsa, E. Hu, S.-H. Yam, and L. Kazovsky, "Performance demonstration of a fast–tunable transmitter and burst–mode packet receiver for HORNET," in *Proc. of OFC 2001*, vol. 4, Anaheim, CA, Mar. 2001, pp. ThG–1–ThG–3.

[5] E. Chan, Q. N. Le, M. Beranek, Y. Huang, D. Koshinz, and H. Hager, "A 12–channel multimode fiber–optic 1.0625–gb/s fiber channel receiver based on COTS devices and MCM-L/COB/BGA packaging," *IEEE Photonics Technology Letters*, vol. 12, pp. 1549–1551, November 2000.

[6] M. Ibsen, S. Alam, M. Zervas, A. Grudinin, and D. Payne, "8- and 16–channel all-fiber DFB laser WDM transmitters with integrated pump redundancy," *IEEE Photonics Technology Letters*, vol. 11, pp. 1114–1116, September 1999.

[7] M. Maier, M. Reisslein, and A. Wolisz, "Towards efficient packet switching metro WDM networks," *Optical Networks Magazine*, vol. 3, no. 6, pp. 44–62, November/December 2002.

[8] B. Mukherjee, "WDM–based local lightwave networks part I: Single–hop systems," *IEEE Network Magazine*, vol. 6, no. 3, pp. 12–27, May 1992.

[9] M. Bandai, S. Shiokawa, and I. Sasase, "Performance analysis of multicasting protocol in WDM–based single–hop lightwave networks," in *Proc. of IEEE Globecom '97*, Phoenix, AZ, Nov. 1997, pp. 561–565.

[10] A. Bianco, G. Galante, E. Leonardi, F. Neri, and A. Nucci, "Scheduling algorithms for multicast traffic in TDM/WDM networks with arbitrary tuning latencies," in *Proc. of IEEE Globecom 2001*, San Antonio, TX, Nov. 2001, pp. 1551–1556.

[11] M. S. Borella and B. Mukherjee, "Limits of multicasting in a packet–switched WDM single–hop local lightwave network," *Journal of High Speed Networks*, vol. 4, pp. 155–167, 1995.

[12] J. P. Jue and B. Mukherjee, "The advantages of partitioning multicast transmissions in a single–hop optical WDM network," in *Proc. of ICC '97*, Montreal, Canada, June 1997.

[13] T. Kitamura, M. Iizuka, and M. Sakuta, "A new partition scheduling algorithm by prioritizing the transmission of multicast packets with less destination address overlap in WDM single–hop networks," in *Proc. of IEEE Globecom*, San Antonio, TX, Nov. 2001.

[14] H.-C. Lin, P.-S. Liu, and H. Chu, "A reservation–based multicast scheduling algorithm with reservation window for single–hop WDM network," in *Proc. of IEEE International Conference of Networks*, Singapore, Sept. 2000.

[15] H.-C. Lin and C.-H. Wang, "A hybrid multicast scheduling algorithm for single–hop WDM networks," *IEEE/OSA Journal of Lightwave Technology*, vol. 19, no. 11, pp. 1654–1664, Nov. 2001.

[16] T.-L. Liu, C.-F. Hsu, and N.-F. Huang, "Multicast QoS traffic scheduling with arbitrary tuning latencies in single–hop WDM networks," in *Proceedings of ICC 2002*, New York, NY, Apr. 2002, pp. 2886–2890.

[17] E. Modiano, "Random algorithms for scheduling multicast traffic in WDM broadcast–and–select networks," *IEEE/ACM Transactions on Networking*, vol. 7, no. 3, pp. 425–434, June 1999.

[18] Z. Ortiz, G. N. Rouskas, and H. G. Perros, "Maximizing multicast throughput in WDM networks with tuning latencies using the virtual receiver concept," *European Transactions on Telecommunications*, vol. 11, no. 1, pp. 63–72, January/February 2000.

[19] G. N. Rouskas and M. H. Ammar, "Multidestination communication over tunable–receiver single–hop WDM networks," *IEEE Journal on Selected Areas in Communications*, vol. 15, no. 3, pp. 501–511, Apr. 1997.

[20] L. Sahasrabuddhe and B. Mukherjee, "Probability distribution of the receiver busy time in a multicasting local lightwave network," in *Proc. of ICC '97*, Montreal, Canada, June 1997.

[21] S.-T. Sheu and C.-P. Huang, "An efficient multicasting protocol for WDM star–coupler networks," in *Proc. of IEEE International Symposium on Computers and Communications*, Alexandria, Egypt, July 1997, pp. 579–583.

[22] W.-Y. Tseng, C.-C. Sue, and S.-Y. Kuo, "Performance analysis for unicast and multicast traffic in broadcast–and–select WDM networks," in *Proc. of IEEE International Symposium on Computers and Communications*, Red Sea, Egypt, July 1999.

[23] A. Ding and G.-S. Poo, "A survey of optical multicast over WDM networks," *Computer Communications*, vol. 26, no. 2, pp. 193–200, Feb. 2003.

[24] A. Hamad and A. Kamal, "A survey of multicasting protocols for broadcast–and-select single–hop networks," *IEEE Network*, vol. 16, pp. 36–48, July/August 2002.

[25] J. He, S.-H. G. Chan, and D. H. K. Tsang, "Multicasting in WDM networks," *IEEE Communications Surveys and Tutorials*, Dec. 2002.

[26] M. McKinnon, G. Rouskas, and H. Perros, "Performance analysis of a photonic single–hop ATM switch architecture, with tunable trasmitters and fixed frequency receivers," *Performance Evaluation*, vol. 33, no. 2, pp. 113–136, July 1998.

[27] L. Wang and K. Lee, "A WDM based virtual bus for universal commuincation and computing systems," in *Proc. of ICC '92*, June 1992, pp. 888–894.

[28] K. Kato, A. Okada, Y. Sakai, K. Noguchi, T. Sakamoto, A. Takahara, A. Kaneko, S. Suzuki, and M. Matsuoka, "10–Tbps full–mesh WDM network based on a cyclic–frequency arrayed–waveguide grating router," in *Proc. of ECOC '00*, vol. 1, Munich, Germany, Sept. 2000, pp. 105–107.

[29] A. Okada, T. Sakamoto, Y. Sakai, K. Noguchi, and M. Matsuoka, "All–optical packet routing by an out–of–band optical label and wavelength conversion in a full–mesh network based on a cyclic–frequency AWG," in *Proc. of OFC 2001 Technical Digest, paper ThG5*, Anaheim, CA, Mar. 2001.

[30] S. B. Alexander, R. Bondurant, D. Byrne, V. Chan, S. Finn, R. Gallager, B. Glance, H. Haus, P. Humblet, R. Jain, I. Kaminow, M. Karol, R. Kennedy, A. Kirby, H. Le, A. Saleh, B. A. Schofield, J. Shapiro, N. Shankaranarayanan, R. Thomas, R. Williamson, and R. Wilson, "A precompetitive consortium on wide-band all-optical networks," *IEEE Journal of Lightwave Technology*, vol. 11, no. 5, pp. 714–735, May/June 1993.

[31] D. Banerjee, J. Frank, and B. Mukherjee, "Passive optical network architecture based on waveguide grating routers," *IEEE Journal on Selected Areas in Communications*, vol. 16, no. 7, pp. 1040–1050, Sept. 1998.

[32] K. Bengi, *Optical Packet Access Protocols for WDM Networks*. Kluwer Academic Publishers, Norwell, MA, 2002.

[33] M. Chia, D. Hunter, I. Andonovic, P. Ball, I. Wright, S. Ferguson, K. Guild, and M. O'Mahony, "Packet loss and delay performance of feedback and feed–forward arrayed–waveguide gratings–based optical packet switches wtih WDM inputs–outputs," *Journal of Lightwave Technology*, vol. 19, pp. 1241–1254, September 2001.

[34] B. Glance, I. P. Kaminow, and R. W. Wilson, "Applications of the integrated waveguide grating router," *IEEE/OSA J. Lightwave Technol.*, vol. 12, no. 6, pp. 957–962, June 1994.

[35] A. Hill, S. Carter, J. Armitage, M. Shabeer, R. Harmon, and P. Rose, "A scalable and switchless optical network structure, employing a single 32×32 free–space grating multiplexer," *IEEE Photonics Technology Letters*, vol. 8, no. 4, pp. 569–571, Apr. 1996.

[36] D. K. Hunter and I. Andonovic, "Approaches to optical Internet packet switching," *IEEE Communications Magazine*, vol. 38, no. 9, pp. 116–122, September 2000.

[37] D. K. Hunter, M. H. M. Nizam, M. C. Chia, I. Andonovic, K. Guild, A. Tzanakaki, M. O'Mahony, L. Bainbridge, M. Stephens, R. Penty, and I. White, "WASPNET: a wavelength switched packet network," *IEEE Communications Magazine*, vol. 37, no. 3, pp. 120–129, March 1999.

[38] D. Jung, S. Shin, C. Lee, and Y. Chung, "Wavelength–division–multiplexed passive optical network based on spectrum–slicing techniques," *IEEE Photonics Technology Letters*, vol. 10, no. 9, pp. 1334–1336, Sept. 1998.

[39] M. J. Karol and B. Glance, "A collision–avoidance WDM optical star network," *Computer Networks and ISDN Systems*, vol. 26, pp. 931–943, Mar. 1994.

[40] M. J. O'Mahony, D. Simeonidou, D. K. Hunter, and A. Tzanakaki, "The application of optical packet switching in future communication networks," *IEEE Communications Magazine*, vol. 39, no. 3, pp. 128–135, March 2001.

[41] M. J. Spencer and M. Summerfield, "WRAP: A medium access control protocol for wavelength–routed passive optical networks," *IEEE/OSA Journal of Lightwave Technology*, vol. 18, no. 12, pp. 1657–1676, Dec. 2000.

[42] A. Bianco, E. Leonardi, M. Mellia, and F. Neri, "Network controller design for SONATA — a large–scale all–

optical passive network," *IEEE Journal on Selected Areas in Communications*, vol. 18, no. 10, pp. 2017–2028, Oct. 2000.

[43] N. P. Caponio, A. M. Hill, F. Neri, and R. Sabella, "Single–layer optical platform based on WDM/TDM multiple access for large–scale 'switchless' networks," *European Transactions on Telecommunications*, vol. 11, no. 1, pp. 73–82, Jan./Feb. 2000.

[44] C. Fan, M. Maier, and M. Reisslein, "The AWG‖PSC network: A performance enhanced single–hop WDM network with heterogeneous protection," in *Proc. of IEEE Infocom*, San Francisco, CA, Mar. 2003, pp. 2279–2289.

[45] A. Hill, M. Brierley, R. Percival, R. Wyatt, D. Pitcher, K. I. Pati, I. Hall, and J.-P. Laude, "Multi–star wavelength–router network and its protection strategy," *IEEE Journal on Selected Areas in Communications*, vol. 16, no. 7, pp. 1134–1145, Sept. 1998.

[46] Y. Sakai, K.Noguchi, R. Yoshimura, T. Sakamoto, A. Okada, and M. Matsuoka, "Management system for full-mesh WDM AWG-STAR network," in *Proc. of ECOC '01.*, vol. 3, Amsterdam, Netherlands, Sept. 2001, pp. 264 –265.

[47] C. Fan, M. Reisslein, and S. Adams, "The $FT^{\Lambda} - FR^{\Lambda}$ AWG network: A practical single-hop metro WDM network for efficient uni- and multicasting," in *Proceedings of IEEE Infocom*, Hong Kong, March 2004.

[48] L. Takacs, *Combinatorial methods in the theory of stochastic processes.* Wiley, 1967.

[49] N. L. Johnson and S. Kotz, *Urn models and their applications.* Wiley, 1977.

[50] K. Park and W. Willinger, Eds., *Self–Similar Network Traffic and Performance Evaluation.* John Wiley & Sons Inc., 2000.